Research Square

Preprints are preliminary reports that have not undergone peer review.
They should not be considered conclusive, used to inform clinical practice,
or referenced by the media as validated information.

# Matrine Exerts Antifungal and Antibiofilm Effects on Candida albicans via the Oxidative Stress-MAPK-Metabolism Axis

**Xiaomin Liu**

78523827@qq.com

The First Affiliated Hospital of Yunnan University of Traditional Chinese Medicine

**Huanqin Li**

The First Affiliated Hospital of Yunnan University of Traditional Chinese Medicine

**Yun Lin**

The First Affiliated Hospital of Yunnan University of Traditional Chinese Medicine

**Yali Bai**

The First Affiliated Hospital of Yunnan University of Traditional Chinese Medicine

**Qin Tang**

The First Affiliated Hospital of Yunnan University of Traditional Chinese Medicine

**Zhiping Yin**

The First Affiliated Hospital of Yunnan University of Traditional Chinese Medicine

**Churong Huang**

The First Affiliated Hospital of Yunnan University of Traditional Chinese Medicine

**Research Article**

**Keywords:** Traditional Chinese medicine, Sophora flavescens, matrine, Candida albicans, oxidative stress, MAPK, metabolomics

**Posted Date:** May 12th, 2026

**DOI:** https://doi.org/10.21203/rs.3.rs-9667972/v1

**License:** This work is licensed under a Creative Commons Attribution 4.0 International License.
Read Full License

**Additional Declarations:** No competing interests reported.

# Abstract

### Aim of the study

Matrine is a major alkaloid component of the traditional Chinese medicinal plant *Sophora flavescens*. Although it has been reported to inhibit fungal growth in vitro, its underlying mechanisms of action and potential molecular targets in *Candida albicans* remain largely unclear. This study aimed to elucidate the antifungal mechanisms of matrine against *C. albicans* using flow cytometry, transcriptomics, and untargeted metabolomics, thereby providing a theoretical basis for further mechanistic and translational research.

### Materials and methods

The ΔOD values were measured with a microplate reader, and the half-maximal inhibitory concentrations ($IC_{50}$) values were calculated by nonlinear regression. The inhibitory effects of matrine were evaluated through time-kill assays, Annexin V-FITC/PI staining, DCFH-DA staining for reactive oxygen species (ROS), cell-cycle analysis, transmission electron microscopy (TEM), and fluorescence-activated cell sorting (FACS). RNA-seq and untargeted metabolomics were employed to explore the underlying antifungal mechanisms, and key pathways and differentially expressed genes were further validated by quantitative real-time PCR (qRT-PCR).

### Results

Nonlinear fitting showed $IC_{50}$ values of 57.79-535.60 μg/mL ($P = 0.0407$), indicating a significant concentration-dependent inhibition. Annexin V-FITC/PI assays showed significant differences in apoptosis between the control and matrine-treated groups at concentrations of 128, 256, and 512 μg/mL (all $P < 0.05$). TEM demonstrated dose-dependent ultrastructural injuries, including cytoplasmic separation, compromised cell-wall architecture, and severe cell-wall disruption and dissolution at concentrations of 512 and 1,024 μg/mL. RNA-seq identified 2,894 differentially expressed genes, including 1,145 upregulated and 1,749 downregulated genes. The upregulation of genes encoding oxidative-stress-related enzymes (*GPX3*, *SOD1*, and *CTT1*) and the unfolded protein response-related transcription factor *HAC1*, coupled with marked alterations in lipid metabolites, strongly suggested that matrine induced profound oxidative stress. Mechanistically, matrine-induced endomembrane injury and lipotoxicity were linked to the dysregulation of genes involved in cell-wall and membrane biosynthesis, including *CHT1* and *FKS2*.

### Conclusion

This study demonstrates that matrine exerts potent antifungal effects against *C. albicans* through an oxidative stress-MAPK-metabolism axis. The proposed mechanism involves the accumulation of ROS, disruption of lipid and redox homeostasis, inhibition of chitin synthase-related cell-wall remodeling (*CHT1*), and modulation of β-1,3-glucan synthase activity (*FKS2*). These cascading effects lead to

impaired cell-wall integrity, disrupted polarized growth, and suppressed hyphal development, providing a mechanistic basis for further development of matrine as a candidate antifungal agent for candidiasis.

# Introduction

Candida spp. are important opportunistic fungal pathogens in humans that commonly colonize moist mucosal and cutaneous sites, including the skin, oral cavity, intestine, and vaginal mucosa. Under normal physiological conditions, this colonization is generally asymptomatic. However, when host immunity is impaired (e.g., in patients with malignancy or receiving immunosuppressive therapy) or when the microbiota balance is disrupted, *Candida* can proliferate and invade mucosal tissues. This can result in oral candidiasis, vulvovaginal candidiasis, superficial skin infections, and, in severe cases, invasive systemic disease[1]. *C. albicans* is among the most common fungal pathogens associated with vaginitis, and its increasing incidence has become an important concern for women's health.

Clinical management of *Candida* infections predominantly relies on a limited repertoire of antifungal classes, such as azoles, polyenes, and echinocandins. However, the clinical use of these agents is limited by their restricted variety, associated toxicities, and the rapid emergence of drug-resistant strains. Therefore, identifying antifungal compounds from natural products has emerged as an important research direction. Traditional Chinese medicine (TCM), with its multi-component and multi-target characteristics and long history of clinical use, offers promising new strategies for antifungal therapy and for mitigating the development of resistance.

The dried root of *Sophora flavescens* Aiton (Ku Shen) is a traditional Chinese medicinal material recorded in the Chinese Pharmacopoeia[2]. It is traditionally described as bitter and cold and is used to clear heat and dry dampness. Classical indications include dysentery, jaundice, eczema, pruritus, scabies, and external treatment of gynecological infections[3–4]. Modern pharmacological studies have shown that *S. flavescens* contains a variety of bioactive constituents, mainly alkaloids and flavonoids[5].

Matrine (C15H24N2O; molecular weight, 248.37) is one of the major alkaloids in *S. flavescens*[6]. Since its isolation and structural characterization, matrine has exhibited a broad spectrum of pharmacological activities, including antitumor, antipyretic, antiviral, and anti-atherosclerotic effects[7–10]. Furthermore, previous studies have also suggested that matrine has broad-spectrum antifungal activity, inhibiting several clinically relevant fungi, including dermatophytes and *C. albicans*[11]. In addition, inhibitory effects against plant pathogenic fungi, such as poplar brown spot fungus and dragon bamboo mildew, have been reported, with IC50 values of 123 μg/mL and 272 μg/mL, respectively[12].

Although existing studies support the in vitro antifungal potential of matrine, its activity against key pathogenic fungi, particularly *C. albicans*, and its deeper mechanisms of action remain insufficiently characterized. Systematic evaluation of the cellular targets and molecular pathways affected by matrine is of theoretical and practical significance for developing this natural product into a potential antifungal agent. Therefore, this study systematically investigated the effects of matrine on *C. albicans* using

Annexin V-FITC/PI staining, DCFH-DA ROS detection, cell-cycle assays, flow cytometry, RNA-seq transcriptomics, and untargeted metabolomics, aiming to clarify its antifungal mechanism.

## Materials and Methods

# Clinical strains and reagents

Clinical non-drug-resistant *C.albicans* strains were obtained from the Clinical Microbiology Laboratory of the First Affiliated Hospital of Yunnan University of Traditional Chinese Medicine. The following reagents and media were used: YPD broth (Mindray); PDA agar and SDA agar (OXOID); 2% glucose; PBS (pH 7.0 ± 0.5; Biosharp); dimethyl sulfoxide (Solarbio); Annexin V-FITC apoptosis detection kit (Thermo Fisher Scientific); DCFH-DA fluorescent probe (2',7'-dichlorodihydrofluorescein diacetate; Thermo Fisher); PI staining solution (Source Leaf); PCR primers (Sangon Biotech, Shanghai, China); RNA fluorescence detection kit (Equalbit RNA BR Assay Kit, Vazyme); HP All-in-One qRT Master Mix II (Kunming Yungen Biology); and 2× Universal Blue SYBR Green qPCR Master Mix (Servicebio). Matrine reference standard (HPLC purity 98%; lot no. 110805–202010) was purchased from the National Institutes for Food and Drug Control of China and dissolved in PBS (pH 7.0 ± 0.5) before use.

## Instruments

The main instruments included a microplate reader (Thermo Multiskan FC), flow cytometer (BD FACSCalibur), DNBSEQ sequencing platform, S1000 thermal cycler, qPCR instrument (Bio-Rad CFX Connect, XLFZ006), electrophoresis apparatus (Bio-Rad, BEP-600), and Q Exactive HF mass spectrometer (Thermo Fisher Scientific, USA).

## Determination of IC / IC and time-kill kinetics

The samples were assigned to three groups with three biological replicates per group: NC, YPD broth (2% glucose) plus drug solution; PC, YPD broth plus diluted fungal suspension; and treatment group, 100 μL of diluted matrine solution plus 100 μL of working fungal suspension. The final fungal concentration was 2 × 10^3 CFU/mL[13]. All samples were incubated in a $CO_2$ incubator at 35°C for 20 h. Absorbance at 600 nm was measured using a microplate reader, and fungal growth inhibition was calculated to determine IC50 and IC90 values.

For time-kill assays, 100 μL aliquots of drug-treated suspension were collected at 0, 2, 4, 6, 8, 10, 12, and 24 h, inoculated onto SDA plates, and incubated at 37°C for 24 h. Fungal colonies were counted, and time-kill curves were generated using GraphPad Prism 8.0 with time on the x-axis and log10 (CFU/mL) on the y-axis.

## Transmission electron microscopy observation

Fungal suspensions were treated with matrine at final concentrations of 0, 512, and 1,024 μg/mL for 20 h. After treatment, cells were digested with low-concentration trypsin, transferred into 1.5-mL EP tubes, fixed in pre-cooled 4.0% fixative for 20 h, embedded in resin, sectioned into 50-nm ultrathin slices, double-stained with uranyl acetate and lead citrate, and observed by Transmission electron microscopy (TEM).

## Flow cytometry

- C.*albicans* cells were cultured in YPD medium and treated with the indicated concentrations of matrine for 20 h. Cells were then collected, stained with Annexin V-FITC/PI, incubated for 10–15 min, and analyzed using a BD FACSCalibur flow cytometer.

# DCFH-DA staining assay

Single-cell suspensions were prepared at 1 × 10^6 cells/mL and stained according to the ROS detection kit protocol using the fluorescent probe DCFH-DA. DCF fluorescence in each sample was quantified with FlowJo to evaluate intracellular ROS levels.

## RNA-seq transcriptomic analysis

Total RNA was extracted from 12 samples (control and treatment groups) and quantified using the Equalbit RNA BR Assay Kit (Vazyme). RNA-seq libraries were analyzed on the DNBSEQ platform. Raw sequencing data were subjected to quality control, and clean reads were aligned and annotated using the Candida Genome Database (CGD).

## Untargeted metabolomic analysis

Metabolites were extracted from two groups and analyzed using an LC-MS platform. Metabolites were annotated using the BMDB (BGI Metabolome Database), mzCloud, and ChemSpider databases. After MS data processing, a data matrix containing metabolite peak areas and identification information was generated. Skyline was used for quantitative analysis, and the Mfuzz R package was used for clustering analysis of metabolite expression profiles across groups.

# Bioinformatic analysis

Weighted gene co-expression network analysis (WGCNA) and pathway enrichment analysis (KEGG + Mummichog algorithm) were performed using R version 4.2.2. Integrated statistical analysis of metabolomics and transcriptomics, including random forest analysis, was performed using R with support from BGI Tech Solution Co.

# qRT-PCR

Total RNA was extracted from each sample and reverse-transcribed using HP All-in-One qRT Master Mix II (RT203-Ver.1). The 20-μL reaction mixture contained 4× All-in-One qRT Master Mix (5 μL), total RNA (2 μg), and RNase-free H2O to 20 μL. After brief centrifugation, reverse transcription was performed in a conventional PCR instrument under the following conditions: 50°C for 10 min, 85°C for 5 s, and 4°C hold.

qPCR was performed using 2× Universal Blue SYBR Green qPCR Master Mix. The reaction mixture contained cDNA (3 μL), 2× Universal Blue SYBR Green qPCR Master Mix (5 μL), forward primer (10 μM, 1 μL), and reverse primer (10 μM, 1 μL). qRT-PCR was conducted on the CFX96 Real-Time PCR Detection System under the following conditions: initial denaturation at 95°C for 10 min; denaturation at 95°C for 15 s; annealing at 60°C for 30 s; and extension at 72°C for 30 s. Amplification and melting curves were collected.

Gene expression was validated by qRT-PCR for targets associated with oxidative stress, the MAPK pathway, peroxisomal membrane components, deoxyribonucleotide biosynthesis, cell cycle regulation, fatty acid metabolism, and secondary metabolite biosynthesis. *18S rRNA*, *ACT1*, and *PMA1* were used as internal reference genes. Primer sequences are listed below:

Table 1
Primer list

| Gene / Direction | | Sequence (5' to 3') | Gene / Direction | | Sequence (5' to 3') |
|---|---|---|---|---|---|
| SOD1 | F | TGGTTGTACTTCTGCTGGTCC | CTT1 | F | AGAGTTGGTCAACACGGTCC |
| | R | CCAATGACACCACAAGCAGG | | R | CACCATAAGCACCGGAACCT |
| HAC1 | F | TGGCTAGACTGATTGCTGCT | CLN1 | F | TGGGGTTACCGGAACCATTG |
| | R | TGACGTCTACACCACCATCT | | R | AGTGGGGATGAAGAGGACGA |
| FAA21 | F | TTGGCATTGGTTCCTCGTGT | CDC28 | F | AGGTGTACCTAGTACCGCCA |
| | R | AGCGATTGGTGCACTACCAG | | R | AGCCCCTAGTCCAACTCCTT |
| PEX11 | F | TGGTTACTTGGTTTAATTGCTGG | CHT1 | F | GACAGACTGGACTGGTGTGG |
| | R | CAGCTAAACCAACATCACCTTCA | | R | GCCCATACCCTGATGAGTCG |
| GLR1 | F | TTCTACCTGCAGCAATGGCA | CYP5 | F | GCCATCTAAGACCTCGCCAA |
| | R | TTCCTCCTTCAGTCCCTGGT | | R | CGTCGAGGAGGATGGCAAAT |
| GPX3 | F | ACCCACTTCACCAGGCTTTT | ACT1 | F | TAGGTTTGGAAGCTGCTGGT |
| | R | GTGGCAAGTTTGTGTGGGTT | | R | ACGTTCAGCAATACCTGGGA |
| PKC1 | F | TTGAACCACCGTATTCCGCA | 18S - rRNA | F | GATCCATTGGAGGGCAAGTCT |
| | R | GAGTATGCCTCGACTCAGCC | | R | CAGACAAATCGCTCCACCAAC |
| FKS2 | F | AGGCCGATAATGCAAACCCA | PMA1 | F | TGTTTTCTTGGCCCCAGGTT |
| | R | ACTTGCTAGCAGTCGCCAAT | | R | GGCCAAAGTGGCAACATCAG |

# Statistical analysis and Bioinformatics analysis

Statistical analysis was performed using GraphPad Prism 9. Using WGCNA weighted gene co-expression network analysis of pathway enrichment (KEGG + Mummichog algorithm) statistical analysis: R language 4.2.2. Statistical Analysis of Metabolomics and Transcriptomics: Implementation of Random Forest Analysis Using R Language. Provided by BGI Tech Solution Co.

## Results

# Drug Control

Matrine (Standards), HPLC 98% (lot: 110805–202010), purchased from China Institute of Food and Drug Identification. Dissolve in PBS, pH 7.0 ± 0.5.

# Determination of $IC_{50}$ /$IC_{90}$ and time-kill kinetics

The NC group showed no microbial growth, whereas the PC group showed fungal growth, confirming assay validity (Table 2). Based on ΔOD values, $IC_{50}$ values were distributed between 64 and 512 μg/mL and $IC_{90}$ values between 128 and 2,048 μg/mL. Nonlinear regression analysis yielded $IC_{50}$ values of 57.79–535.60 μg/mL (Table 2, Table 3). These results indicate that matrine inhibited *C. albicans* growth in vitro in different culture media, with inhibition increasing as the drug concentration increased. Differences from the control group were statistically significant (P = 0.0001 and P = 0.0006; P < 0.05) (Fig. 2,Fig. 3).

Table 2
In vitro inhibition of *C. albicans* by matrine in different culture media

| **Sample** | **Concentration (μg/mL)** | | | |
|---|---|---|---|---|
| | **2,048 μg/mL** | **1,024 μg/mL** | **NC** | **Positive control** |
| F46 | 0.066 | 0.057 | 0.075 | 0.121 |
| T67 | 0.061 | 0.065 | 0.065 | 0.109 |
| F34 | 0.077 | 0.069 | 0.078 | 0.142 |
| T50 | 0.074 | 0.070 | 0.075 | 0.146 |

Table 3
$IC_{50}$ and $IC_{90}$ values calculated by nonlinear fitting

| **$IC_{50}$ (μg/mL)** | **F64** | **T67** | **F34** | **T50** |
|---|---|---|---|---|
| | **>64** | **>256** | **512** | **> 128** |
| Nonlinear-fit $IC_{50}$ (μg/mL) / log(inhibitor) vs. response -- variable slope (four parameters) | 57.79 | 401.70 | 535.60 | — |
| $IC_{90}$ (μg/mL) | 128 | 1024 | 1024 | 512 |

Table 3
Average colony counts (CFU/mL) at different matrine concentrations and time points

| Concentration (μg/mL) | 0h | 2h | 4h | 6h | 8h | 10h | 12h | 24h |
|---|---|---|---|---|---|---|---|---|
| 512 | 58 | 24.2 | 24.4 | 28.3 | 13.0 | 20.7 | 3.5 | 0.5 |
| 256 | 58 | 23.6 | 24.2 | 79.8 | 31.7 | 28.5 | 70.0 | 621.6 |
| 128 | 81 | 21.2 | 16.6 | 39.7 | 157.9 | 716.7 | 533.3 | > 1000(≈ 3.0×10^4) |
| 64 | 56 | 18.9 | 11.5 | 16.4 | 149.2 | 266.7 | 1100.0 | > 1000(≈ 7.5×10^4) |
| PC | 65.6 | 12.4 | 7.0 | 74.2 | 348.0 | 1333.3 | 1566.7 | > 1000(≈ 1.7×10^5) |
| NC | 0 | 0 | 0 | 0 | 0 | 0 | 0 | 0 |

# Transmission electron microscopy observation of *C. albicans* ultrastructure after matrine treatment

The NC group exhibited intact cell walls, cell membranes, and overall cellular morphology, with no obvious swelling or damage. In the 1,024 μg/mL group, most cells showed membrane separation, incomplete cell-wall structures, and occasional cell damage. Structural damage in the 512 μg/mL group was less severe than that in the 1,024 μg/mL group, and more cells retained relatively complete morphology(Fig. 4). Overall, matrine caused concentration-dependent destruction of *C. albicans* cellular structures.

# Flow cytometric evaluation of the antifungal effects of matrine

*C. albicans* infected cells were cultured in YPD medium and treated with the indicated concentrations of matrine for 20 h. Cells were then collected, stained with Annexin V-FITC/PI, incubated for 10–15 min, and analyzed using a BD FACSCalibur flow cytometer. Flow analysis showed that the proportion of viable cells (Q4) decreased gradually with increasing matrine concentration, whereas necrotic/apoptotic cells (Q2 and Q3) increased. Compared with the control group, the treatment groups (128, 256, and 512 μg/mL) showed significant differences ($P < 0.0002$, $P = 0.0001$, and $P = 0.0001$, respectively; all $P < 0.05$; Fig. 5).

# DCFH-DA staining assay for reactive oxygen species accumulation in *C. albicans*

Flow cytometric analysis showed that the proportion of ROS-positive cells increased in the 2,048 μg/mL group. Because ROS accumulation can promote apoptosis, these results suggest that matrine affects *C. albicans* cellular processes and apoptosis partly through ROS generation (Table 4 and Fig. 6). At 512 μg/mL, the number of *C. albicans* cells decreased and most cells showed yeast-like morphology. By contrast, the negative control group displayed branched hyphal forms, indicating that matrine suppressed hyphal growth and may exert antibiofilm activity. Hyphal formation is closely associated with pathogenicity and tissue invasion by *C. albicans* (Fig. 7).

Table 4
DCFH-DA fluorescence analysis of intracellular ROS

| Group | NC | 1,024 μg/mL | 2,048 μg/mL |
|---|---|---|---|
| Value of DCF+ | 4.07% | 4.34% | 11.0% |
| | 4.38% | 4.07% | 11.2% |
| | 4.29% | 4.40% | 11.3% |
| | 4.53% | 2.98% | 16.5% |
| | 4.00% | 2.73% | 15.8% |
| | 3.78% | 3.02% | 15.4% |
| | 1.97% | 5.17% | 9.32% |
| | 2.31% | 5.06% | 9.83% |
| | 2.25% | 5.20% | 9.15% |
| Mean ± SD | 3.51 ± 1.03% | 4.11 ± 0.98% | 12.17 ± 2.92% |

(Experimental groups A-C: 1,024, 512, and 256 μg/mL; D, NC).

# RNA-seq transcriptomic analysis

In the C.albicans RNA-seq dataset, 12,231 genes were identified with > 80% alignment coverage. Group differences were assessed using a t-test based on 2^-ΔCT data; fold change was calculated from the ratio of 2^-ΔCT values between groups. Genes with $|\log_2 FC| \geq 1$ and $P < 0.05$ were defined as significantly differentially expressed. A total of 2,894 DEGs were identified, including 1,145 upregulated and 1,749 downregulated genes (Fig. 7A).

GO enrichment analysis revealed that DEGs between the matrine-treated and NC groups were mainly associated with plasma membrane components, membrane-associated structures, extracellular regions, extracellular vesicles, the cell surface, the mitochondrial respiratory chain, and the fungal cell wall. In the biological process category, DEGs were enriched in arginine biosynthesis, cellular iron ion homeostasis, iron ion transport, carbohydrate transport, copper ion import, inositol biosynthesis, dicarboxylic acid transport, siderophore transport, glutathione membrane transport, and asparagine catabolism. In the

molecular function category, DEGs were enriched in carbohydrate binding, ferric-chelate reductase activity, argininosuccinate synthase activity, inositol-3-phosphate synthase activity, dicarboxylic acid transmembrane transporter activity, 4-α-hydroxytetrahydrobiopterin dehydratase activity, and asparaginase activity (Fig. 7B,7C).

These transcriptomic findings were consistent with the TEM observations, both indicating that matrine affects the membrane and cell-wall structures of *C. albicans*.

KEGG enrichment analysis was performed using KOBAS, and the 20 most significantly enriched pathways are shown in Fig. 7D. DEGs between the treatment and NC groups were mapped to 115 signaling pathways, of which 21 were significant ($P < 0.05$). The enriched pathways included ribosome biogenesis, sulfur metabolism, alanine/aspartate/glutamate metabolism, glutathione metabolism, arginine biosynthesis, tyrosine metabolism, pyruvate metabolism, and peroxisome-related pathways.

# Untargeted metabolomic analysis

# Statistical method

Differential metabolites between groups were screened using univariate and multivariate analyses. PCA and PLS-DA were first performed to evaluate overall group separation, and OPLS-DA was then used to calculate variable importance in projection (VIP) values. Differential metabolites were defined as those meeting the following criteria: VIP ≥ 1 in the OPLS-DA model, fold change ≥ 1.2 or ≤ 0.83, and q-value < 0.05. Classification plots, volcano plots, and other visualizations were generated (Fig. 8A). PCA was used to assess the distribution and separation trends between groups, including inter-group and intra-group variation (Fig. 8A).

# Analysis

A total of 16,472 compounds were identified, of which 3,640 could be classified (Fig. 7B). These compounds mainly included terpenoids, flavonoids, coumarins and derivatives, alkaloids and derivatives, lipids, benzene and derivatives, amino acids, peptides and analogues, organic acids, carbohydrates, and other metabolites. Among them, 491 metabolites were significantly altered, including 242 upregulated and 249 downregulated metabolites (Fig. 7B).

The differential metabolites were mainly enriched in amino acid metabolism, xenobiotic biodegradation, carbohydrate and nucleotide metabolism, lipid metabolism, secondary metabolite biosynthesis, and cofactor/vitamin metabolism. Amino acid metabolism was one of the most active metabolic pathways in the current samples (Fig. 8C).

Lipid metabolism is central to *C. albicans* cell-membrane homeostasis(Table 5). Lipid classes such as ergosterol (a classical antifungal drug target), sphingolipids, glycerolipids, and phospholipids are essential for membrane fluidity, lipid homeostasis/lipotoxicity [14], signal transduction, energy metabolism, growth and reproduction, pathogenicity, and drug resistance [15, 16].(Fig. 8D). The

accumulation of lipid metabolic products suggests that matrine affects cell-membrane and cell-wall stability, a conclusion supported by the TEM observations.

Figure 8. Untargeted metabolomic analysis(A: Permutation test plot of the PLS-DA model for group comparison (treated vs. negative control)(Blue dots represent results from 1,000 random permutations; the red line represents the regression line of permuted data; the red solid circle indicates the original model. R2Y = 0.98; Q2 intercept = -0.08; P < 0.001); B: Volcano plot of differential metabolite analysis(A, volcano plot; B, number of metabolites; C, metabolic pathway classification); C: Overall metabolite classification; D: Heat map of read counts)

Table 5
Metabolic pathway enrichment analysis

| KEGG pathway | Number of metabolites | P value | Rich factor |
|---|---|---|---|
| Biosynthesis of secondary metabolites | 35 | 7.13E-05 | 0.0155 |
| Biosynthesis of amino acids | 11 | 6.20E-09 | 0.0859 |
| ABC transporters | 9 | 1.62E-06 | 0.0652 |
| D-Amino acid metabolism | 7 | 1.26E-06 | 0.1014 |
| Arginine and proline metabolism | 7 | 1.26E-06 | 0.1014 |

# Real-time fluorescence PCR validation based on Bio-Rad CFX 96

To assess consistency between omics findings and gene expression, differential genes were validated by qRT-PCR, and 2^-ΔΔCT values across samples were visualized using clustered heat maps. Data were standardized using Z-scores to represent relative expression levels. Validation focused on pathways related to oxidative stress response and protection, peroxisomes and peroxisomal membrane components, MAPK signaling, steroid biosynthesis, cell-cycle regulation, deoxyribonucleotide biosynthesis, fungal ribosome biosynthesis, metabolism, antioxidant/reductive reactions, fatty acid, carbohydrate, and energy metabolism, and amino acid biosynthesis. The expression levels of HAC1, SOD1, GPX3, and CTT1 were elevated, indicating oxidative stress in Candida cells after matrine treatment and supporting the ROS assay results. Matrine also inhibited the expression/activity of CHT1 chitin synthase and FKS2 β-1,3-D-glucan synthase, and decreased CLN1 expression, consistent with cell-cycle arrest in the G0/G1 and G2/M phases (Fig. 8).

## Discussion

*S. flavescens* is a traditional Chinese medicine used for conditions such as dysentery, hematochezia, jaundice, urinary retention, leukorrhea, genital swelling and itching, eczema, sores, pruritus, boils, tinea,

leprosy, and external treatment of trichomonas vaginitis. Matrine, one of its main active compounds, is also present in several traditional Chinese medicine formulations and may contribute important synergistic effects. However, its antifungal mechanism has not been fully clarified. In this study, nonlinear regression indicated that the $IC_{50}$ of matrine against *C. albicans* was 57.79–535.60 μg/mL and the $IC_{90}$ was 128-1,024 μg/mL. These values differed from the previously reported $IC_{50}$ of 3.125 μg/mL [11], which may be related to differences in strains, media, assay conditions, or calculation methods.

The effects of matrine on *C. albicans* viability were evaluated using Annexin V-FITC/PI staining and BD flow cytometry. FlowJo analysis showed significant differences compared with the control group ($P < 0.0001$, $P = 0.0001$, and $P = 0.0002$), supporting the antifungal activity of matrine.

TEM observations showed that matrine-treated cells exhibited membrane separation, incomplete cell-wall structures, and occasional cell-wall rupture and dissolution. The extent of structural damage increased with increasing matrine concentration. Pathogenic fungi such as *C. albicans* can undergo apoptosis-like cell death in response to adverse stimuli [17, 18]. Necrosis and apoptosis represent important forms of cell death, characterized by cell swelling, loss of plasma membrane integrity, leakage of cellular contents, disruption of ion gradients, or genetically regulated programmed cell death. Our results are consistent with these processes.

DCFH-DA staining showed that intracellular ROS levels in *C. albicans* increased with matrine concentration. Statistical analysis showed that the ROS-positive proportion in the 2,048 μg/mL group increased approximately fourfold compared with the untreated group ($P < 0.0001$). Increased ROS production was accompanied by reduced fungal growth and suppressed hyphal formation. ROS, as a second messenger, plays an important role in apoptosis and necrosis [19]. Under physiological conditions, ROS participates in energy metabolism and cell proliferation; however, excessive ROS accumulation disrupts the oxidative-antioxidative balance, damages macromolecules such as DNA and proteins, and promotes programmed cell death [20]. High ROS levels may also impair mitochondria and reduce mitochondrial membrane potential, an early indicator of apoptosis [21]. Similar findings have been reported for TTS-12, a compound extracted from *Tribulus terrestris*, which induces *C. albicans* apoptosis by increasing intracellular ROS levels [22].

Excessive ROS can attack membrane lipids and generate lipid radicals. These highly reactive lipid peroxidation products may amplify damage through peroxisomal metabolic pathways, fatty acid oxidation, and acetyl-CoA transferase-associated metabolism. Therefore, matrine may broadly impair the cytoplasmic membrane system, plasma membrane components, extracellular region, extracellular vesicles, cell surface, and fungal cell-wall biosynthesis. Such chain reactions can damage the plasma membrane and may ultimately lead to cell death [23].

Transcriptomic, metabolomic, and qRT-PCR analyses confirmed increased expression of HAC1, SOD1, and GPX3, supporting the occurrence of oxidative stress in Candida cells after matrine treatment. This result is consistent with the ROS assay. HAC1 is a transcription factor associated with endoplasmic

reticulum stress, whereas GPX3 encodes a glutathione peroxidase that helps reduce $H_2O_2$ to $H_2O$ and $O_2$ through the glutathione (GSH) system and contributes to antioxidant defense.

SOD1 encodes superoxide dismutase, a key enzyme involved in scavenging superoxide anions. CTT1 encodes peroxisomal catalase, which helps prevent intracellular lipid peroxidation, limits organic peroxide formation, and protects cells from oxidative lipid damage. The upregulation of HAC1, SOD1, GPX3, and CTT1 after matrine treatment suggests activation of an oxidative-stress defense response and indicates that ROS-mediated injury may be an important contributor to the antifungal activity of matrine.

FAA21, an acyl-CoA synthetase, participates in lipid synthesis and fatty acid oxidation. In lipid metabolism, FAA21 regulates acyl-CoA pool partitioning by activating medium- and long-chain fatty acids, promoting peroxisomal oxidative energy production, and reducing intracellular free fatty acid accumulation to maintain membrane lipid homeostasis and energy balance. During oxidative stress, FAA21 may enhance antioxidant capacity by decreasing lipotoxic ROS generation, supporting NADPH-dependent GSH recycling, and stabilizing membrane lipid fluidity. Conversely, loss of FAA21 function can cause fatty acid accumulation, mitochondrial dysfunction, ROS bursts, membrane damage, and cell death. In *C. albicans*, FAA21 activity is related to growth, biofilm formation, adhesion/invasion, virulence, and susceptibility to antifungal agents [24].

Glutathione reductase GLR1 is mainly localized in mitochondria and reduces oxidized glutathione (GSSG) to reduced glutathione (GSH) in an NADPH-dependent manner, thereby maintaining glutathione homeostasis. PEX11 encodes a peroxisomal membrane protein involved in peroxisome division, fusion, and abundance regulation; it also participates in fatty acid oxidation and antioxidant defense, contributing to ROS clearance and redox balance. The decreased expression of GLR1 and PEX11 suggests impairment of the antioxidant defense system [25].

Under matrine treatment, increased ROS production, reduced ROS-scavenging capacity, and disrupted redox homeostasis may cause extensive endomembrane and cell-wall damage, potentially activating the yeast MAPK cascade. The MAPK signaling pathway participates in Candida cell-wall damage repair, osmotic stress homeostasis, nutrient-stress responses, expression of cell-wall-related genes, maintenance of cell-wall integrity, actin cytoskeleton organization, targeted vesicle secretion to growth sites, β-glucan synthesis, spore formation, pseudohyphal growth, and cell-cycle regulation. This pathway is therefore important for signal transduction and apoptosis-related responses in *C. albicans*. In the canonical cascade, multiple receptors activate BCK1 through phosphorylation; BCK1 then activates Mkk1/2, which further phosphorylates MPK1. Activated MPK1 enters the nucleus to regulate transcription factors such as RLM1, thereby controlling DNA transcription and influencing cell-wall integrity and remodeling, including processes related to FKS2-encoded β-glucan synthesis.

FKS2 encodes a catalytic subunit involved in the biosynthesis of major cell-wall glucans, including β-1,3-glucan and β-1,6-glucan, which account for approximately 50%-60% of the cell wall [26, 27]. These

components are essential for maintaining cell integrity and for cell-wall remodeling, bud-tip polarized growth, and cytoplasmic development during budding. The Candida cell wall is a layered structure that accounts for 20%-30% of the dry cell weight and supports cell shape, osmotic pressure, material exchange, nutrition, proliferation, and budding reproduction. The outer layer mainly consists of highly glycosylated mannoproteins, whereas the inner layer contains glucan polymers, chitin, and small amounts of transmembrane proteins. Glucan and chitin account for most of the inner wall mass, and β-1,3-glucan chains with β-1,6-linked branches constitute a major part of this structure [28, 29].

Chitin is a major component of cell-wall-anchored proteins and is also associated with the cytoplasmic membrane system. Previous studies suggest that chitin contributes to vesicle secretion, budding growth, and membrane development in Candida [30], whereas chitin deficiency can cause septum formation defects and even growth arrest [31]. Reduced synthesis of chitin and β-1,3-D-glucan may alter fungal osmotic pressure and lead to cell-wall rupture or cell death. In this study, the activity/expression of chitin synthases CHT1 and CHS2 was significantly inhibited.

TEM results showed that 20 h of matrine treatment caused varying degrees of cell-wall rupture and structural deficiency, indicating that matrine impaired the structure and function of the fungal cell wall, disrupted cell-wall integrity, or inhibited cell-wall synthesis. These observations were supported by RNA-seq and qRT-PCR results.

Through this pathway, PKC1, β-1,3-glucan synthase (HGT12/GS), BNI1 and SKN7 transcription factors, the GTP-Rho-binding vesicle subunit SEC3, FKS2, and chitin synthases CHT1 and CHS2 jointly participate in glucan/chitin synthesis and cell-wall repair (Fig. 16). These genes are important markers of cell-wall biogenesis [32, 33, 34].

In summary, this study demonstrates that matrine exerts antifungal effects against *C. albicans* through the oxidative stress-MAPK-metabolism axis. The proposed mechanism involves inhibition of chitin synthase-related processes (CHT1), impairment of cell-wall/membrane development and hyphal growth, and disruption of cell-wall repair through modulation of FKS2-associated β-1,3-glucan synthesis. These findings provide a mechanistic basis for further investigation of matrine as a potential therapeutic strategy for candidiasis.

## Declarations

# Author Contribution

1.The following financial interests/personal relationships considered as potential competing interests This study was supported by the Funding of Applied Basic Research Foundation of Yunnan Province (CN) (NO.202501AT070487) This study was supported by the Joint Fund of Yunnan University of Traditional Chinese Medicine and the First Affiliated Hospital (NO.XYLH202009) This study was supported by the Applied Basic Research Foundation of Yunnan Province (NO.XYLH202301AZO70001-

144 This study was Suppored by the Joint Found of Yunnan University of Traditional Chinese Medicine and the First Affiliated Hospital (NO.XYLH202215) The drugs, or supplies was provided by China Food and Drug Inspection Institute (Beijing). Equipment for drug validation was supported by the Experimental Research Center of Yunnan Provincial Hospital of Traditional Chinese Medicine This study statistical analysis was provided by Wuhan China University. Huang Churong reports a relationship with Yunnan College of Business Management that includes: non-financial support. 2.CRediT authorship contribution statement Liu Xiaomin: Writing – original draft, review & editing, Methodology, Data curation, Conceptualization. Huang Churong: Writing – original draft, Writing – review, Data curation.Li Huanqing: Methodology, Data curation. Bai Yali: MethodologyData curation. Tang Qin: Writing – review, Conceptualization, Supervision. Lin Yun: Methodology, Conceptualization, Supervision. Yin Zhiping: Supervision

## References

1. Donnelly JP, Chen SC, the Mycoses Study Group Education and Research Consortium [J]. Revision and Update of the Consensus Definitions of Invasive Fungal Disease From the European Organization for Research and Treatment of Cancer and. Clin Infect Dis. 2020;71(6):1367–76. 10.1093/cid/ciz1008. . PMID: 31802125; PMCID: PMC7486838.
2. Zeng Yuan'er. China Pharmacopoeia 2010 (Part I) Concise Manual of Chemical Composition Analysis [M]. Sun Yat-sen University; 2010.
3. Wang Jiaokui Z. Ruixian. Research on the Shen Nong Ben Cao Jing [M]. Beijing: Science and Technology; 2001.
4. Tao Hongjing. Collected Annotations on the Classic of Materia Medica [J]. Qunlian Publishing House; 1955.
5. Xi Y, Guanghuan S, Linlin C, et al. Synthesis and Activity of Berberine Derivatives: A Review of Recent Advances [J]. Synthesis Chem. 2024;32(4):381–92.
6. JUANES M, SARAGI R T, ENRíQUEZ L, et al. Molecular rotation spectrum of tetracyclic quinolizidines: observation of trans-matrine and the elusive cisn-matrine [J]. J Org Chem. 2021;86(2):1861–7.
7. Zhang Zhongwei L, Jieying H, Liang, et al. Study on the Effects and Mechanisms of Berberine on the Proliferation, Apoptosis, and Migration of Lung Cancer Cells A549 [J]. J Youjiang Minzu Med Coll. 2024;46(01):13–7.
8. Chen Linjin X, Yingyu C. The cell cycle regulation mechanism of oxalicine regulating the CDK4/cyclinD1 pathway to induce apoptosis in prostate cancer PC-3 cells [J]. China J Gerontol. 2024;44(02):490–3.
9. Jianjun J. Qiu Wenkui. The pro-apoptotic mechanism of oxalicine via mitochondrial autophagy mediated by COX-2/PINK1/Parkin signaling pathway in MG63 osteosarcoma cells [J]. China Pharm. 2024;35(01):44–50.
10. Li X, Lu Y, Wen P, Yuan Y, Xiao Z, Shi H, Feng E. Matrine restrains the development of colorectal cancer through regulating the AGRN/Wnt/β-catenin pathway [J]. Environ Toxicol. 2023;38(4):809–

19. 10.1002/tox.23730. . Epub 2023 Jan 9. PMID: 36620879.

11. Hua GS, Tao F, Yuanyuan L et al. Study on the In Vitro Antifungal Activity of Theobromine [J]. New Traditional Chinese Medicine and Clinical Pharmacology, 2011,22(4):382–385.
12. Yang Xueyun Z, Boguang JY. The Antibacterial Activity and Synergistic Effects of Sophorine and Oxidized Sophorine [J]. J Nanjing Forestry Univ (Natural Sci Edition), 2008, (02):79–82.
13. Bertout S, Dunyach, Drakulovski P, et al. Comparison of the Sensititre YeastOne dilution method with the Clinical Laboratory Standards Institute (CLSI) M27-A3 microbroth dilution reference method for determining MIC of eight antifungal agents on 102 yeast strains [J]. Pathol Biol (Paris). 2011;59(1):48–51. 10.1016/j.patbio.2010.07.020.
14. Davis J. Glycerolipid homeostasis in Candida albicans, its role in virulence, and the potential for lipotoxicity as an anti-biofilm therapeutic [D]. Kent Acad Repos. 2025;4. 10.13140/RG.2.2.14272.18352.
15. Anonymous. Kinase mediated regulation of lipid metabolism and the crosstalk with drug tolerance mechanisms in Candida albicans [J]. J Med Sci Sports Pharm. 2020;245–52. 10.3844/jmssp.2020.245.252.
16. Garbe E, Gerwien F, Driesch D, Müller T, Böttcher B, Gräler M, Vylkova S. Systematic Metabolic Profiling Identifies De Novo Sphingolipid Synthesis as Hypha Associated and Essential for Candida albicans Filamentation [J]. mBio. 2022;13(6):e02255–22. 10.1128/mbio.02255-22.
17. Madeo F, Herker E, Wissing S, Jungwirth H, Eisenberg T, Fröhlich KU. Apoptosis in yeast [J]. Curr Opin Microbiol. 2004;7(6):655–60.
18. Yang, Yi, Ning Yumei. Modern Research Progress on the Apoptosis Mechanism of Candida albicans [J]. Western J Traditional Chin Med. 2012;25(1):4.
19. Rinnerthaler M, Büttner S, Laun P, et al. Yno1p/Aim14p, a NADPH-oxidase ortholog,controls extramitochondrial reactive oxygen species generation, apoptosis, and actin cable formation in yeast [J]. Proc Natl Acad Sci USA. 2019;109(22):8658–63.
20. Litemburg-Apers DC, Willems PH, Koopman WJ, et al. Interactions between mitochondrial reactive oxygen species and cellular glucose metabolism [J]. Arch Toxicol. 2015;89:1209–26.
21. Brooks MM, Neelam S, Fudala R, et al. Lenticular mitoprotection. Part A: Monitoring mitochondrial depolarization with JC-1 and artifactual fluorescence by the glycogen synthase kinase-3 β inhibitor [J]. Mol Vis. 2019;19:1406–12.
22. Huang Shan Y, Ying. Jiang Yuan Ying. Effects of Natural Compound TTS-12 on Apoptosis of Candida albicans Cells [J]. Armed Police Med J. 2011;22(1):27–33.
23. Rinnerthaler M, Büttner S, Laun P, et al. Yno1p/Aim14p, a NADPH-oxidase ortholog,controls extramitochondrial reactive oxygen species generation, apoptosis, and actin cable formation in yeast 24. [J]. Proc Natl Acad Sci USA. 2019;109(22):8658–63.
24. Kamiryo T, Mishina M, Tashiro SI, Numa S. Candida lipolytica mutants defective in an acyl-coenzyme A synthetase: isolation and fatty acid metabolism [J]. Proc Natl Acad Sci USA. 1977;74(11):4947–50.

25. García-Leiro A, Cerdán ME, González-Siso MI. A functional analysis of Kluyveromyces lactis glutathione reductase [J]. Yeast. 2010;27(7):431 – 41. 10.1002/yea.1760. PMID: 20148387.
26. Gow NA, Hube B. Candida albicans cell wall glycobiology and virulence [J]. Nat Rev Microbiol. 2012;10(2):112–22.
27. Li Min C, Yun S. Isolation, purification, and analysis of alkali-soluble β-glucan from the cell wall of Candida albicans [J]. Chin J Dermatology. 2000;33(5):311–3.
28. Mayor S, Riezman H. Sorting GPI-anchored proteins [J]. Nat Rev Mol Cell Biol. 2004;5(2):110–20. 10.1038/nrm1309.
29. Levin DE. 2005. Cell Wall Integrity Signaling in Saccharomyces cerevisiae [J]. Microbiol Mol Biol Rev 69.
30. Selvaggini S. Independent regulation of chitin synthase and chitinase activity in Candida albicans and Saccharomyces cerevisiae[J]. Microbiology. 2004;150(4):921–8. 10.1099/mic.0.26661-0.
31. WINTER MUNROCA, BUCHAN K, HENRY A, BECKER K, BROWN JM, BULAWA CE AJP. Chs1 of Candida albicans is an essential chitin synthase required for synthesis of the septum and for cell integrity[J]. Mol Microbiol. 2004;39(5):1414–26.
32. Van Drogen F, Dard N, Pelet S, Lee SS, Mishra R, Srejić N, Peter M. Crosstalk and spatiotemporal regulation between stress-induced MAP kinase pathways and pheromone signaling in budding yeast [J]. Cell Cycle. 2020;19(14):1707–15.
33. Fonzi WA. The protein secretory pathway of Candida albicans [J]. Mycoses. 2009;52(4):291–303. 10.1111/j.1439-0507.2008.01673. xIF: 3.1 Q2. Epub 2009 Jan 21. PMID: 19207839.
34. Bishop A, Lane R, Beniston R, Chapa-y-Lazo B, Smythe C, Sudbery P. Hyphal growth in Candida albicans requires the phosphorylation of Sec2 by the Cdc28-Ccn1/Hgc1 kinase [J]. EMBO J. 2010;29(17):2930–42. 10.1038/emboj.2010.158. . Epub 2010 Jul 16. PMID: 20639857; PMCID: PMC2944046.

# Figures

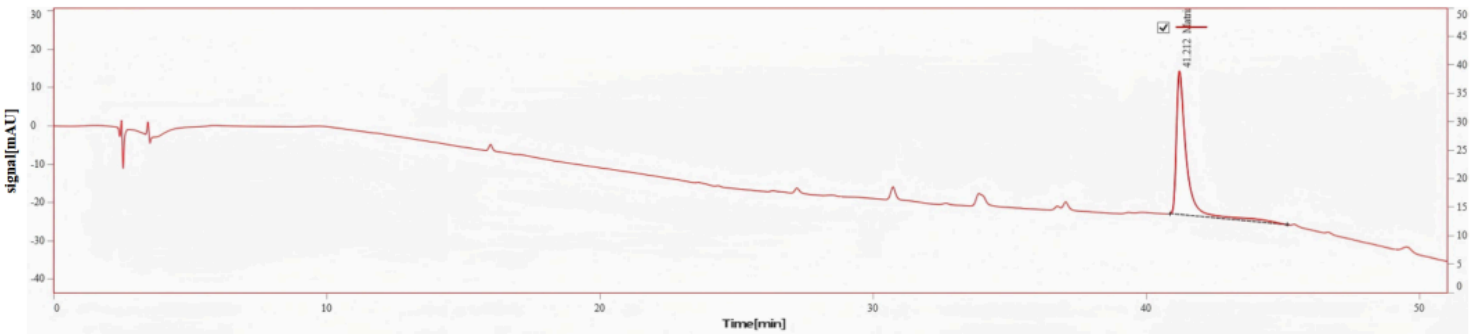
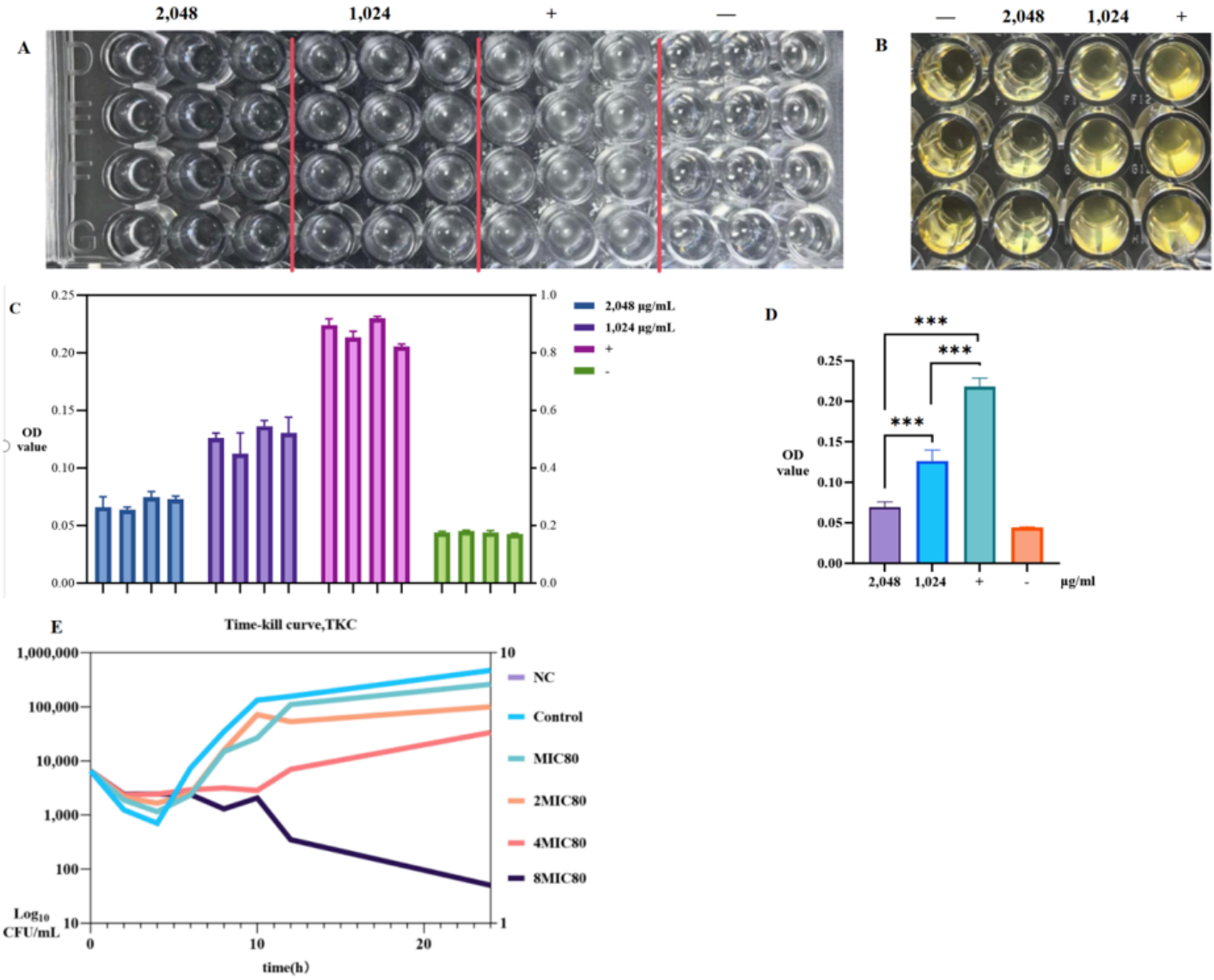



**Figure 1**

Content Analysis of Matrine, HPLC-FLD




## Figure 2

In vitro inhibition of C. albicans by matrine in different culture media

(A, YPD with 2% glucose in PBS, pH 7.0 ± 0.5; B, PDA with 2% glucose in PBS, pH 7.0 ± 0.5).

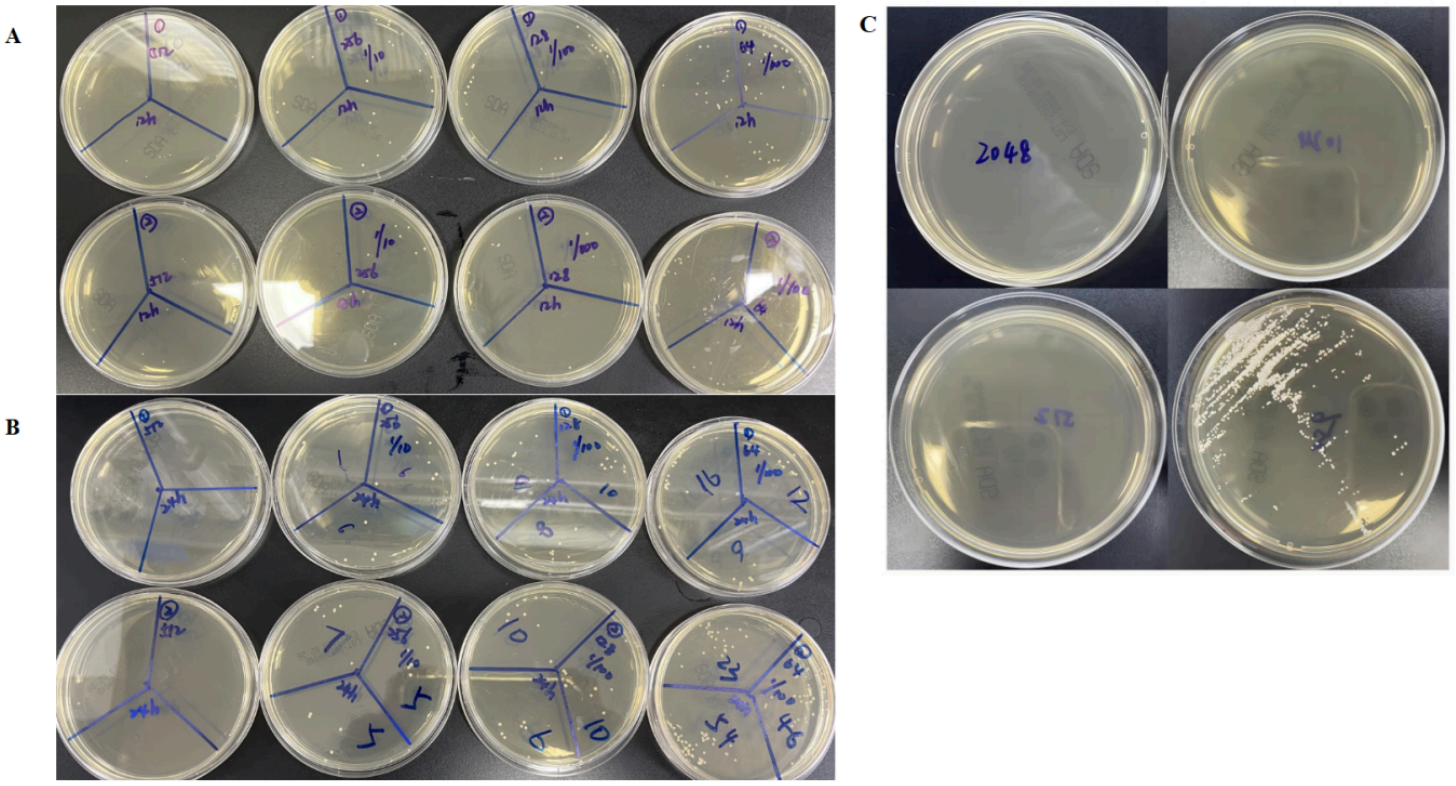
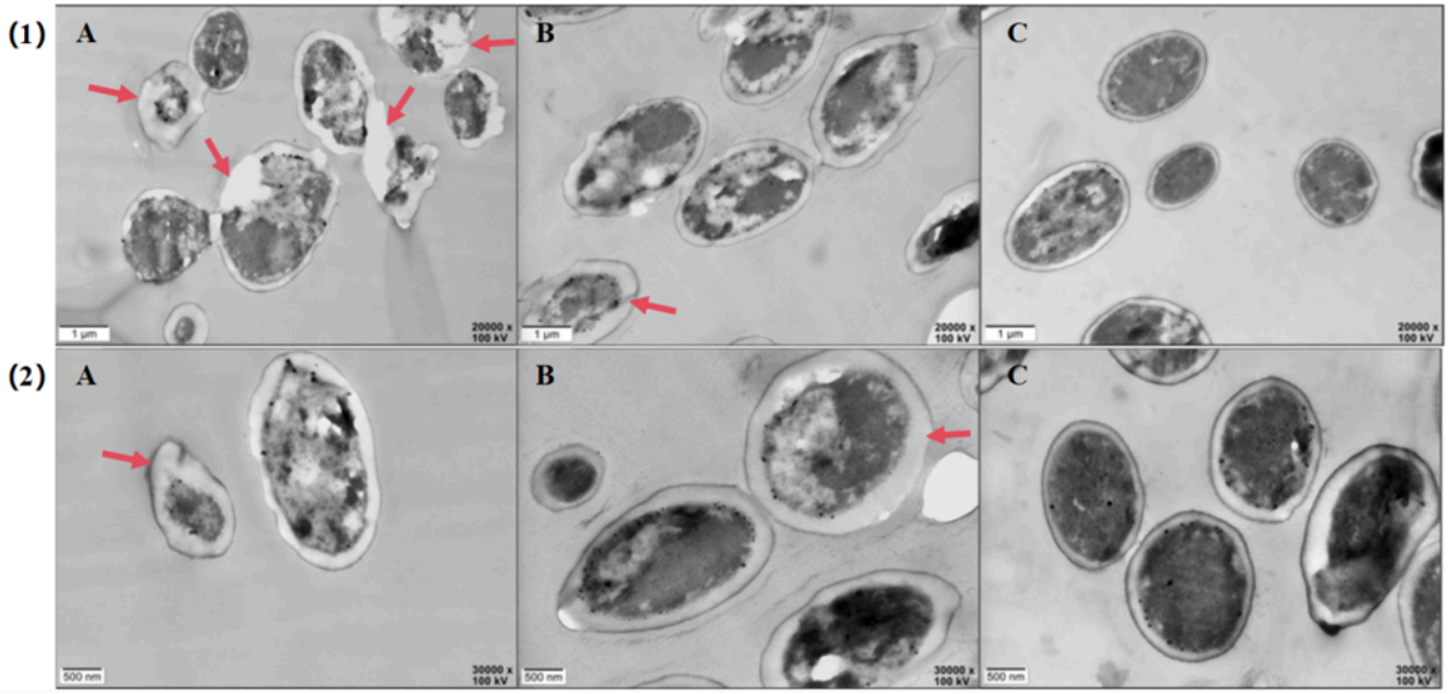



**Figure 3**

Growth dynamics of C. albicans under matrine treatment

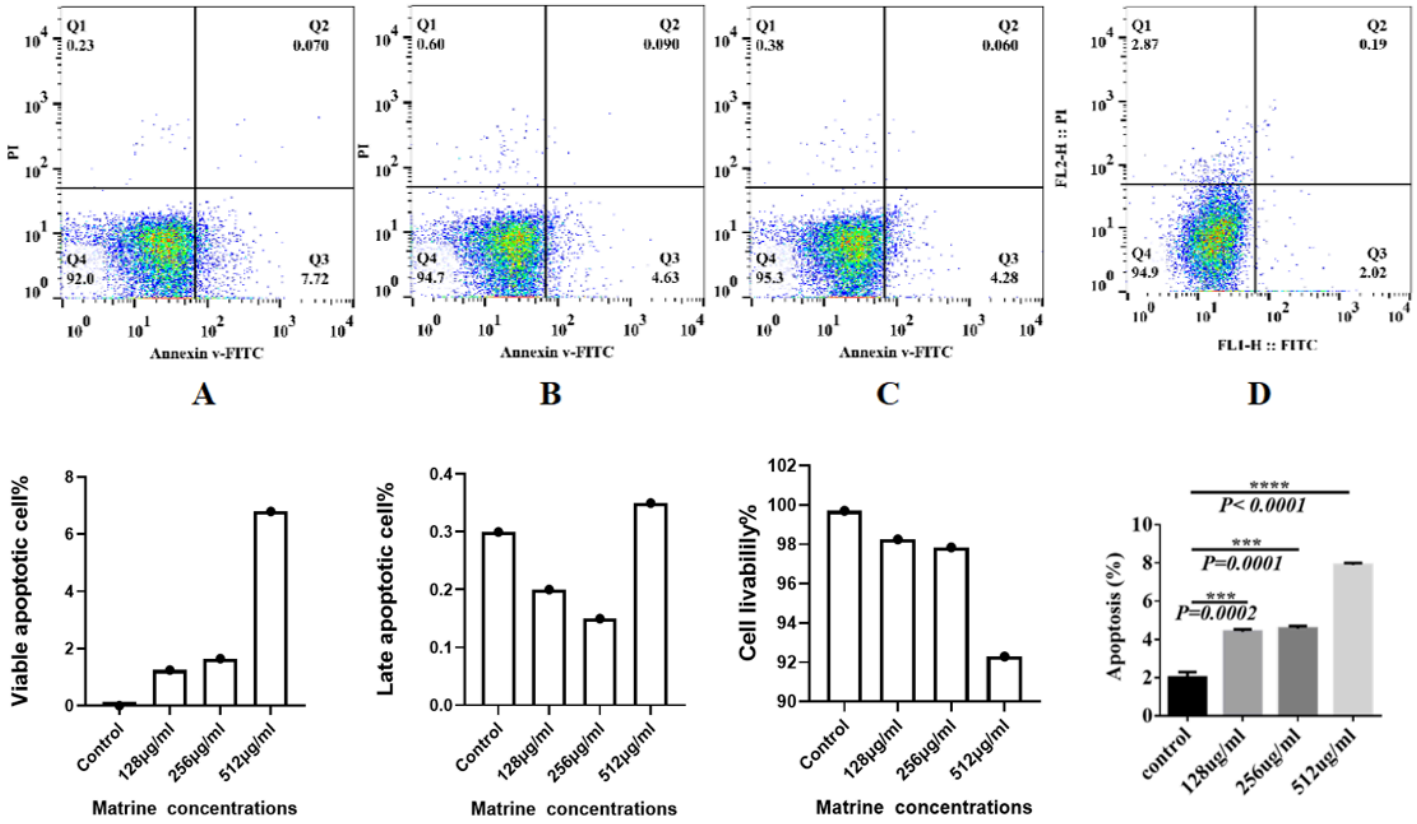
(A, matrine treatment for 12 h: 512, 256 (1/10), 128 (1/100), and 64 (1/100) μg/mL; B, matrine treatment for 24 h: 512, 256 (1/10), 128 (1/100), and 64 (1/100) μg/mL; C, matrine treatment for 24 h: 2,048, 1,024, 512, and 256 μg/mL).



## Figure 4

Effects of matrine on the ultrastructure of C. albicans: (1) 20,000×; (2) 30,000×

(A, 1,024 μg/mL; B, 512 μg/mL; C, NC).




## Figure 5

Annexin V-FITC/PI staining analysis

(A, 512 μg/mL; B, 256 μg/mL; C, 128 μg/mL; D, NC).

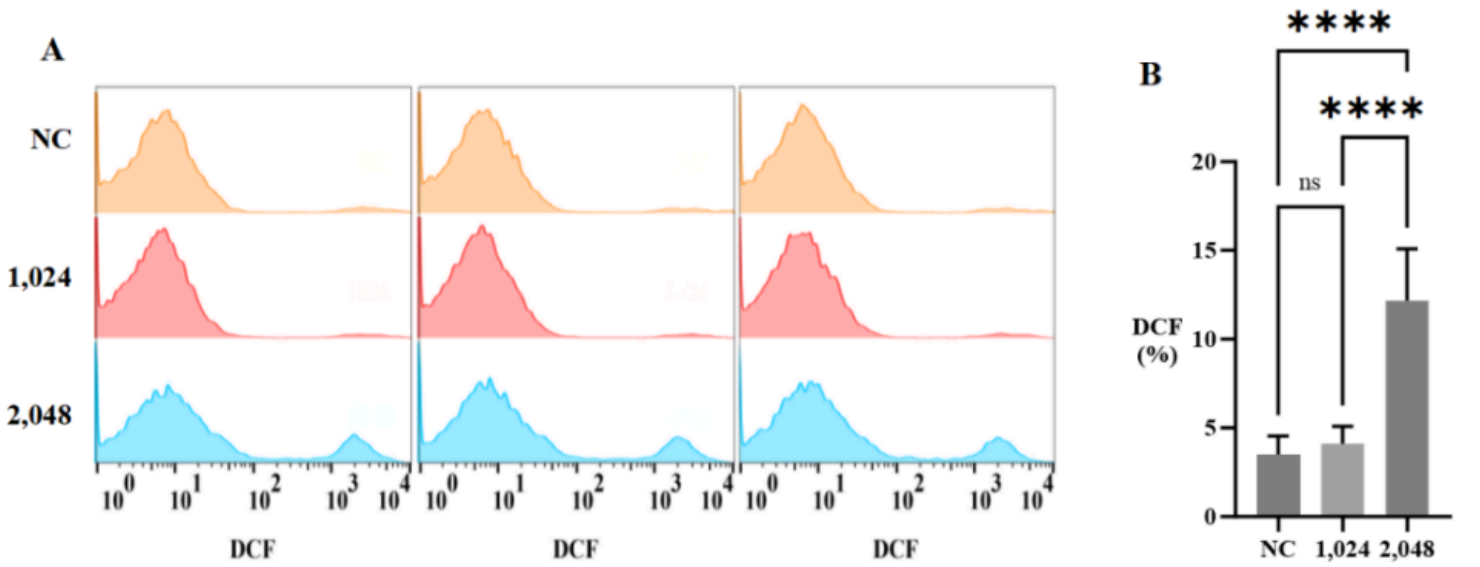



**Figure 6**

FACSCalibur flow cytometric analysis

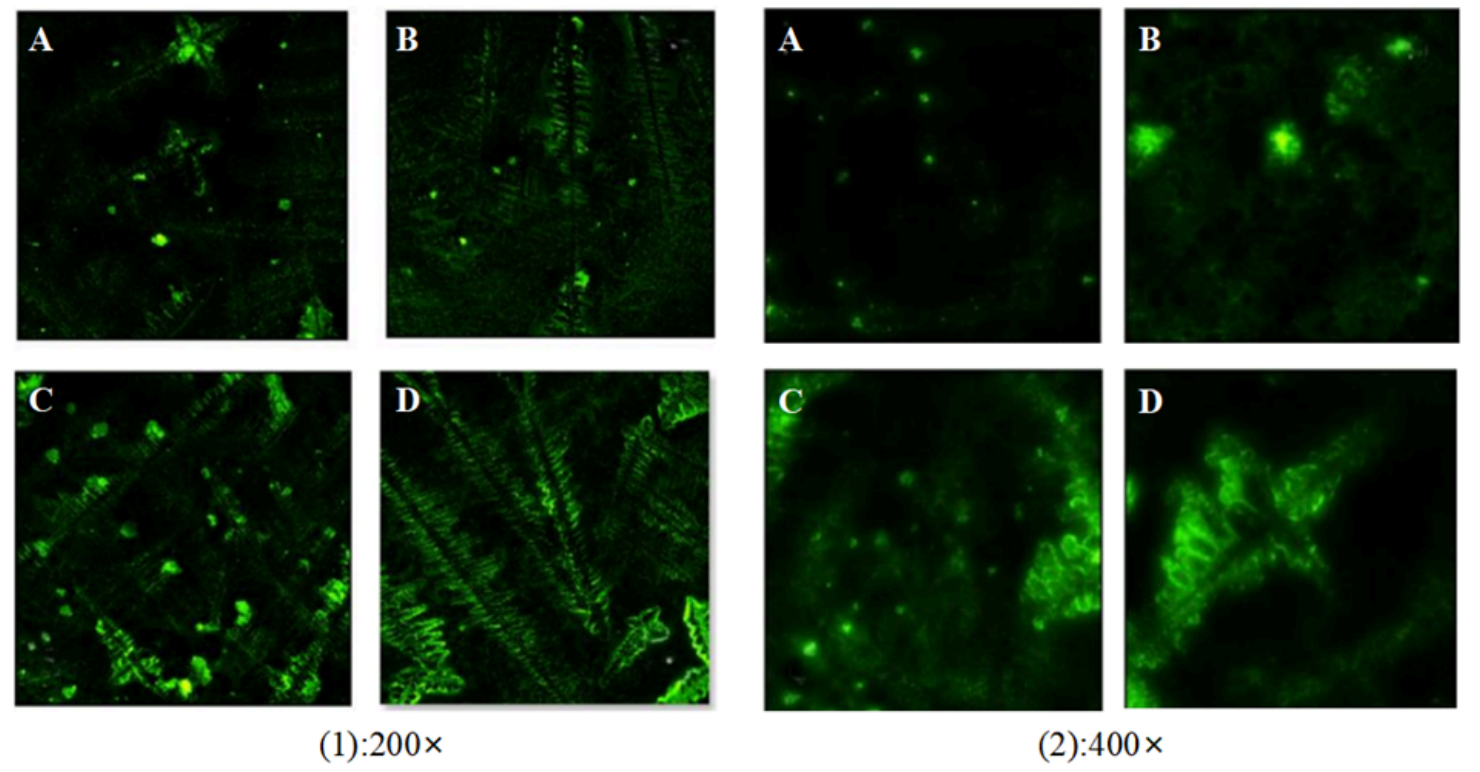



**Figure 7**

ROS assay showing intracellular reactive oxygen species in C. albicans

(Experimental groups A-C: 1,024, 512, and 256 μg/mL; D, NC).

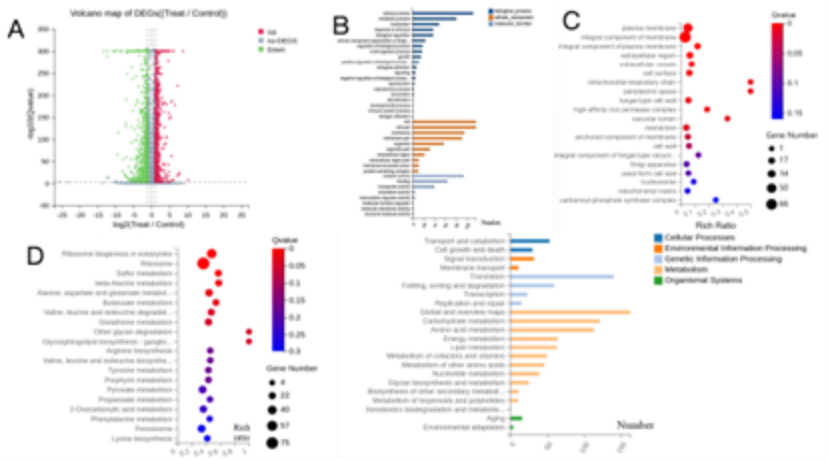


**Figure 8**

Figure 7. RNA-Seq transcriptome analysis of C. albicans infected cells (A: differential gene enrichment analysis; B: GO annotation classification; C: GO cellular component enrichment; D: KEGG pathway enrichment analysis and Classification)

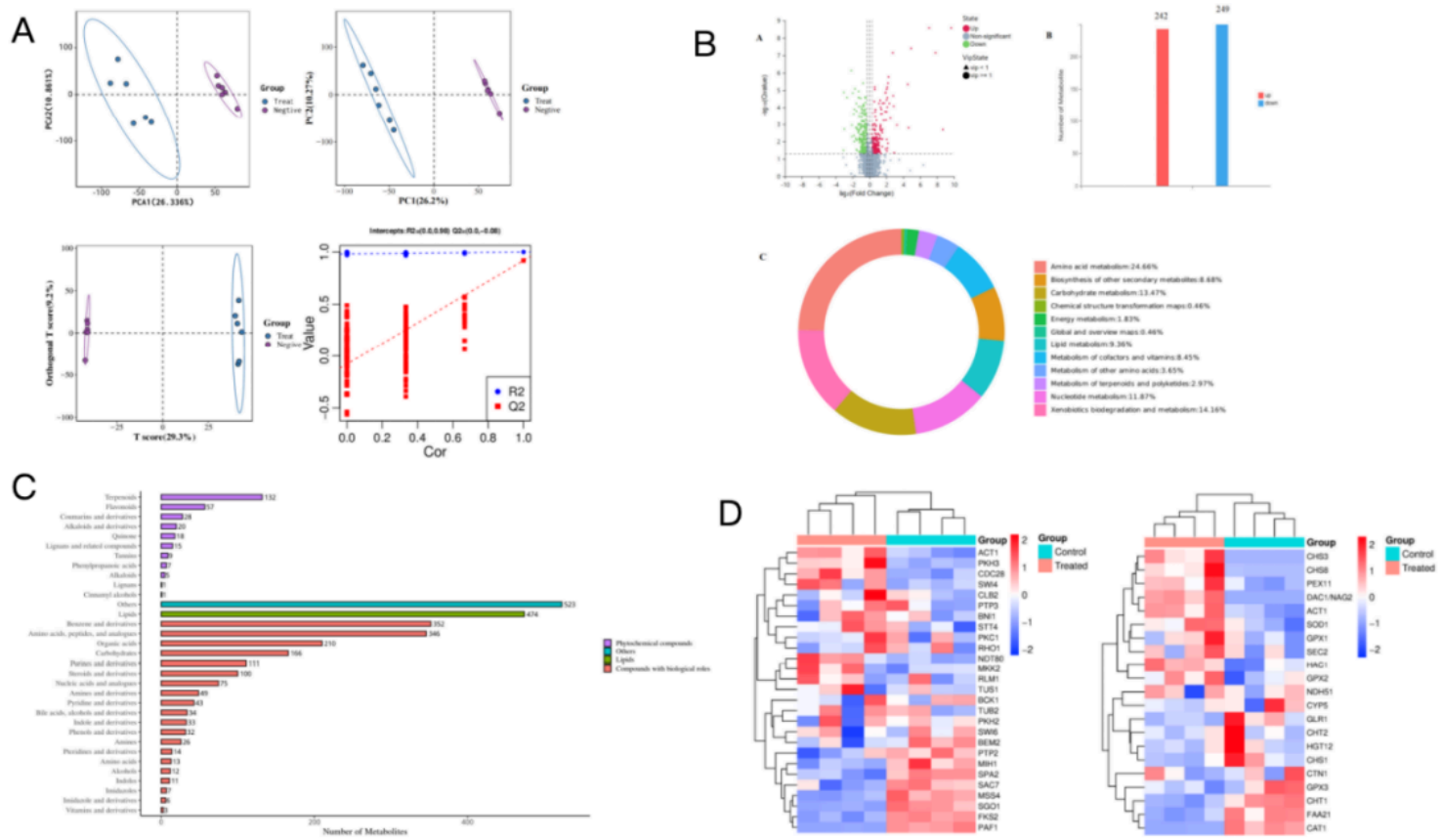


**Figure 9**

Figure 8. Untargeted metabolomic analysis(A: Permutation test plot of the PLS-DA model for group comparison (treated vs. negative control)(Blue dots represent results from 1,000 random permutations; the red line represents the regression line of permuted data; the red solid circle indicates the original

model. R2Y = 0.98; Q2 intercept = -0.08; P < 0.001); B: Volcano plot of differential metabolite analysis(A, volcano plot; B, number of metabolites; C, metabolic pathway classification); C: Overall metabolite classification; D: Heat map of read counts)

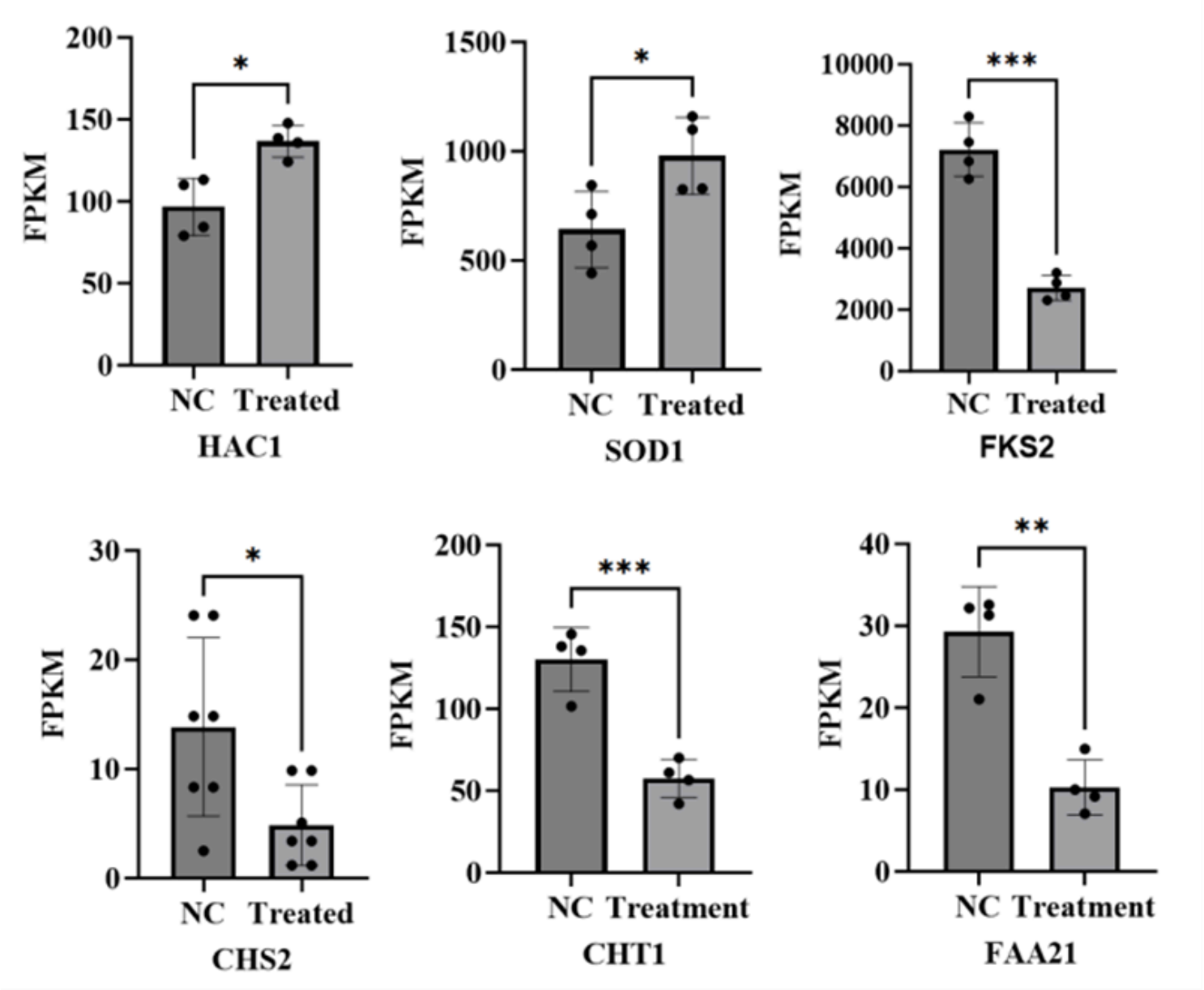



**Figure 10**

Figure 9. Differential expression

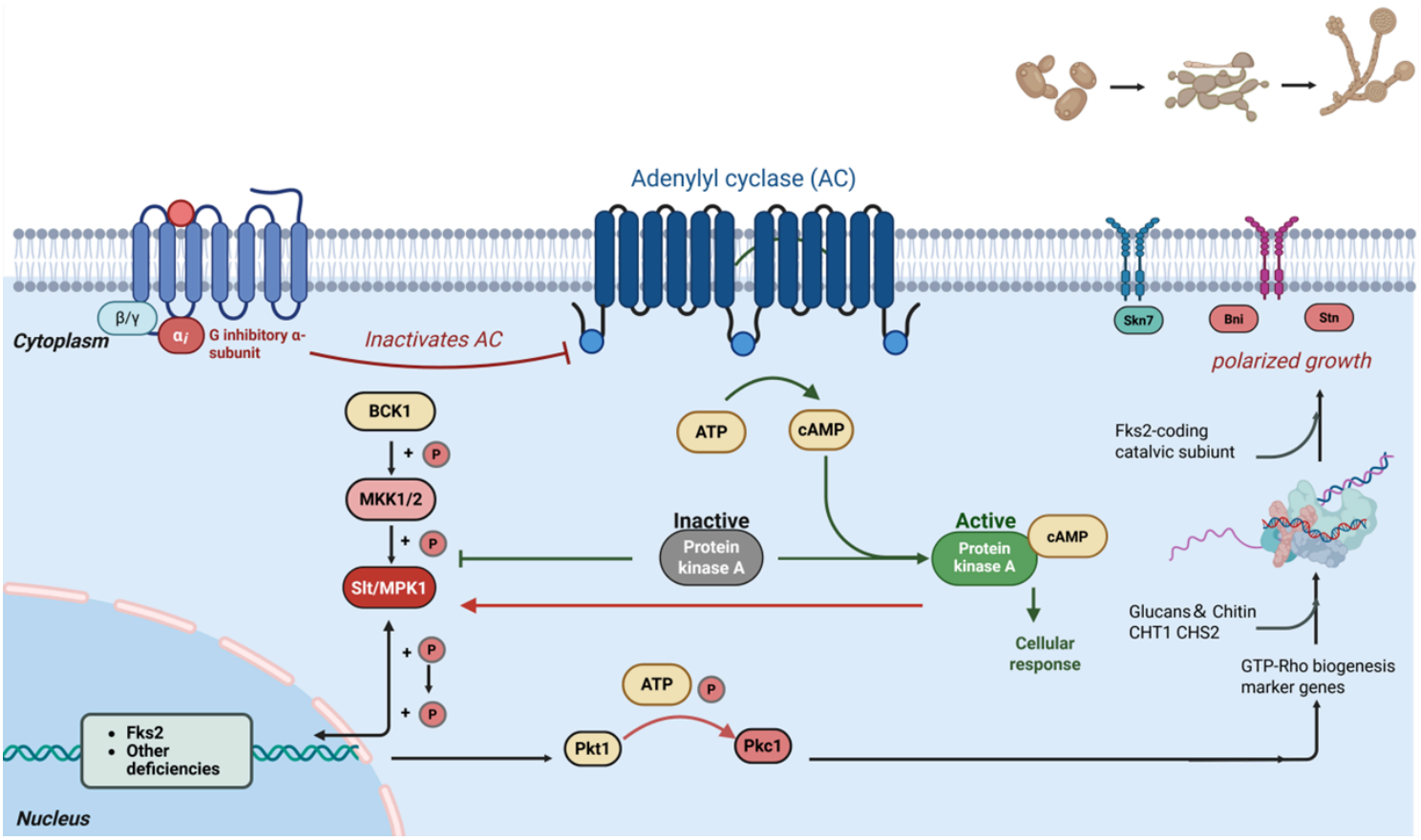



**Figure 11**

Figure 9. Proposed mechanism of matrine against *C. albicans*.Under the action of the drug sophoridine, the production of ROS (reactive oxygen species) in fungal cells increases, the clearance ability weakens, and the ability to maintain redox balance declines, resulting in extensive damage to the inner membrane and cell wall, which may trigger the MAPK (yeast) cascade reaction. The MAPK cascade reaction is sensed by multiple receptors and is inhibited by phosphorylation, thereby inhibiting the phosphorylation activation of Mkk1/2 mitogen-activated protein kinase and the phosphorylation activation of Slt2 (MPK1). Eventually, the expression levels of GTP-Rho-related genes decrease. The inhibition of FKS2 and Chitinase genes CHT1 and CHS2 leads to the occurrence of fungal cell wall repair and Polarized growth disorders). *The map adapted from the 'Activation of Protein Kinase A [PKA]' template; created with BioRender.*

## Supplementary Files

This is a list of supplementary files associated with this preprint. Click to download.

- declarationStatement.docx